Review

A Review of Friction Dissipative Beam to Column Connections for Seismic Design of MRFs

Piero Colajanni *, Muhammad Ahmed, Salvatore Pagnotta *, Pietro Orlando

Posted Date: 26 December 2023

doi: 10.20944/preprints202312.1958.v1

Keywords: Beam-to-Column Connection; Friction; Energy Dissipation; Seismic Energy

 doi:10.20944/preprints202312.1958.v1

Review

A Review of Friction Dissipative Beam to Column Connections for Seismic Design of MRFs

Piero Colajanni [1,*], Muhammad Ahmed [2] and Salvatore Pagnotta [3,*], Pietro Orlando [4]

[1] Department of Engineering, University of Palermo; piero.colajanni@unipa.it
[2] Department of Engineering, University of Palermo; muhammad.ahmed@unipa.it
[3] Department of Engineering, University of Palermo; salvatore.pagnotta@unipa.it
[4] Department of Engineering, University of Palermo; pietro.orlando@unipa.it
* Correspondence: P.C. piero.colajanni@unipa.it; S.P. salvatore.pagnotta@unipa.it

Abstract: The use of friction-based Beam-to-Column Connections (BCC)s for earthquake-resistant Moment Resistant Frames (MRFs), aiming at eliminating damage to beam end sections due to the development of plastic hinges, has taken hold since the early eighties. Different technical solutions were proposed for steel structures, some were also designed for timber structures, while few more recent studies concern friction joints employed in reinforced concrete structures. Research aimed at characterizing the behavior of joints has focused on the evaluation of the tribological properties of the friction materials, coefficient of friction, shape and stability of the hysteresis cycles, influence of the temperature, speed of load application, effects of the application method, stability of preload, the influence of seismic excitation characteristics on the structural response, statistical characterization of amplitude and frequency of the slip excursion during seismic excitation. Studies aimed at identifying the design parameters capable of optimizing performance have focused attention mainly on the slip threshold, device stiffness, and deformation capacity. This review compiles the main and most recent solutions developed for MRFs. Furthermore, the pros and cons for each solution are highlighted, focusing on the dissipative capacity, shape and stability of hysteresis loops. In addition, the common issues affecting all friction connections, namely characteristics of friction shims and the role of bolt preload, are discussed. Based on the above considerations, a guideline can be outlined, which can help to choose the appropriate solutions for beam-to-column connections for MRFs.

Keywords: Beam-to-Column Connection; Friction; Energy Dissipation; Seismic Energy

1. Introduction

Since many decades engineers are trying to protect structures from hazardous seismic events by establishing effective design and retrofitting strategies. [1] placed the foundations of seismic design based on the energy balance between energy transmitted by the earthquake (input energy), and energy absorbed and dissipated by the structure. In order to reduce the energy transmitted to the structure, seismic isolation devices can placed at the base of structure (base isolation system BIS) [2], or vibrating barriers (ViBa)s can be buried in the soil, detached from surrounding buildings that exploiting the soil structure interaction (SSI) and are able to absorb a large rate of the seismic energy transferred by the ground motion [3]. Thus, the limitation of the input energy requires complex devices that modifies the structural behavior, and therefore require advanced design criteria. In more conventional framed system design practice, an appropriate calibration of the overall stiffness and resistance of the structure can allow a modest reduction in input energy [4]. Thus, the most common anti-seismic design techniques are oriented towards providing the structure with characteristics and devices capable of dissipating energy transmitted with limited damage [5]. Main energy dissipation source for standard Moment Resisting Frames (MRFs) according to capacity design approach is to provide by plastic hinges at beam-to-column connections. To avoid beam end damage, to increase the dissipation capacity, moderate the energy and displacement seismic demand, the use of additional energy dissipation devices inside [6] or outside [7] the structure was proposed and investigated.

 doi:10.20944/preprints202312.1958.v1

The reason why so many innovative solutions for beam to-column connections have been developed for steel structures over the last 25 years lies in the poor performance of some of them showed during Northridge (1994) and Kobe (1995) destructive earthquakes. These events represented a game-changer for the structural engineers' community. As a matter of fact, pre-Northridge beam-to-column connections of steel MRFs were usually realized by welding beam flanges on column flange. The plastic hinge was supposed to form starting from the welds connecting beam and column. This constructional detail led to unpredicted stress concentration causing numerous premature failures and limited connection ductility. For this reason, all post Northridge connections have the common goal of avoiding any damage to the elements connecting beam and column. With regard to energy dissipation, this can be ensured, for instance, by formation of ordinary plastic hinge in beam segment sufficiently distanced by column flange, and characterized by dogbone section, or by introducing innovative systems. This type of solution, although limiting fragile breakages due to the presence of welds, does not protect the beam from damage caused by exceeding the elastic limit, allowing a potential accumulation of damage capable of leading the element to collapse due to low-cyclic fatigue. Therefore, solutions that involved the concentration of damage in special portion of the beam specifically designed [8–10] or in devices suitably added with the aim of dissipating energy, which had already been proposed since the seventies [6], began to become increasingly successful.

Supplementary energy dissipation devices are grouped into two broad categories: hysteretic devices with displacement-dependent behavior, and devices with velocity dependent behavior, such as viscoelastic and fluid viscous one.

Hysteretic devices with displacement-dependent behavior are widely studied and adopted in the construction sector, since they appear to be the simpler types of dampers. Their performance is not significantly influenced by the loading amplitude, frequency, operating temperature, and only to a limited extent by the number of cycles [11,12]. Hysteretic dissipation in the mechanics field can be obtained from two main distinct sources: plastic behavior or friction, namely metallic or friction damper. Recently, devices linked to the use of shape memory alloys have become increasingly successful [13,14].

The use of friction dampers placed within the bracing were investigated by [15], on the basis of working phenomenon same as of automotive braking. These friction dampers activate or start yielding before the yielding of main components of the structure. So, in other words these friction dampers work on the principle of braking instead of breaking [16,17]. The friction dampers dissipate more energy than normal hysteretic devices because of the well-developed rectangular force displacement hysteretic loops as reported in [18,19]. Also, friction dampers have a repeatable behavior, higher initial stiffness, and early energy dissipation under small displacement [20,21]. Thanks to their great versatility into wide application fields, these dampers can be used in simple Moment Resisting Frames (MRFs) to aviation and mechanical industry [22–24]. Friction dampers can also be used in conjunction with other dampers like viscoelastic dampers [25] and with metallic damper [19,26–30] etc.

Research on the use of dissipative devices for seismic protection of buildings can be divided into two large groups. In the first, the designed devices and their behavior are described in detail, obtained experimentally or numerically through analysis with the FEM. In the second, the seismic behavior of the structures in which they are inserted is analyzed. In the first area, the key research topics are the tribological behavior of the friction material used, the methods of application and control of the preload applied to the devices that generate it (generally bolts), the design solutions used to create the device, the shape and stability of the resulting hysteresis loops, and the recentering capacity of the devices. In the second area, fundamental research topics are interconnected with each other like the identification of the optimal values of the stiffness and resistance of the device (the latter expressed as optimal slip load), the distributions of the latter in plans and in elevation in the structure, the positions in which to place the device, and the prediction of performance in relation to the characteristics of the earthquake.

Here, attention is paid on the first research field, with the aim of narrowing the interest on devices for beam to column connection in seismic design of MRFs. However, some experimental

 doi:10.20944/preprints202312.1958.v1

results regarding the behavior of the whole structure are also reported [31], aiming at highlighting the potential sources of device damage by tests on large-scale structures.

In this field, since the pioneer paper is of [6], many solutions were proposed for steel MRFs; more recently some were also designed for timber [32] and reinforced concrete precast structures [33], while some recent solutions were proposed for RC columns cast in situ connected with hybrid steel trussed concrete beams (HSTCB)s [34].

To describe recent developments into the design of friction devices for beam to column connection, this review paper is divided in to two sections. The first part describes some of the most relevant technical solutions designed, focusing on the global behavior of the devices. These are grouped into four different categories depending on the layout of the dissipative system:

- asymmetric connections with one or more friction shims to one side only
- asymmetric connections with one or more friction shims per side
- symmetric connections with additional steel element(s) and two or more friction shims
- symmetric connections with two or more friction shims per side

The connection is defined symmetric if the steel plates which transfer the friction forces between beam and column are arranged to obtain aligned resultant forces (so that the bolts are not subjected to prying forces).

The second part of the paper addresses the common factors affecting the performance of friction-based beam to column devices. Thus, firstly the emphasis is on the role of the friction materials (brass, steel, thermal sprayed aluminum) [35]. Then, the factors affecting the performance of the devices, mainly the methods of application (torque wrench) and control (disc spring) of the bolt preload are analyzed. Both of aforementioned are usually investigated by testing uniaxial friction dissipative devices.

2. Rotational Slotted Bolted Connection

One of the first solutions proposed for friction devices applied at beam-to column joints, was reported in [36,37] and belongs to the fourth group (Figure 1a). The system is constituted by two T stubs, each of these bolted to the beam flanges and covered by a cap plate. At each interface T stub-beam flange and T stub-cap plate is inserted a friction shim. Beam web is bolted to the column flange via vertical steel angles, in which the central bolt acts as the center of rotation, while the other bolts are inserted through slotted holes.

The advantage of this solution is that, having a properly defined center of rotation, the kinematic of the connection is readily predictable. However, the position of the center of rotation causes a sensible gap opening during rotation between column flange and top beam flange, leading to potential damage to the slab. In addition, particular attention should be given to the design of the bolt representing the center of rotation, named pivot bolt, as well as the plates connected by it.

As a matter of fact, the first of the two specimens tested by [37] showed that no element constituting the connection was damaged at the end of the test, except for the pivot bolt, whose shank was bent by shear. In addition, reversed cyclic action enlarged the hole on the beam web through which the pivot bolt was inserted. For this reason, for the second specimen was adopted a larger pivot bolt and the beam web was reinforced.

Experimental tests employed brass as friction shim material. The results showed that, despite the brass provided exceptionally stable cyclic behavior, as shown in Figure 1b, its friction coefficient was quite low and required to build a connection with many friction surfaces and bolts to obtain a proper moment strength. Furthermore, the moment of the connection during sliding phase showed a slight hardening behavior.

This can be explained by the fact that, once the connection started to rotate, T stubs were bent, and the bending moment acting on them contributed to increase the moment of the whole connection. With regard to the shape of corners of hysteresis loops, this is due to the slippage of brass pads during load reversal, caused by clearance hole.

 doi:10.20944/preprints202312.1958.v1

Despite the several flaws affecting the proposed solution, it can be stated that the tested connections behaved outstandingly well. It is worth remembering that this solution was pioneer and the application of such friction connections to structural engineering was at the very beginning.

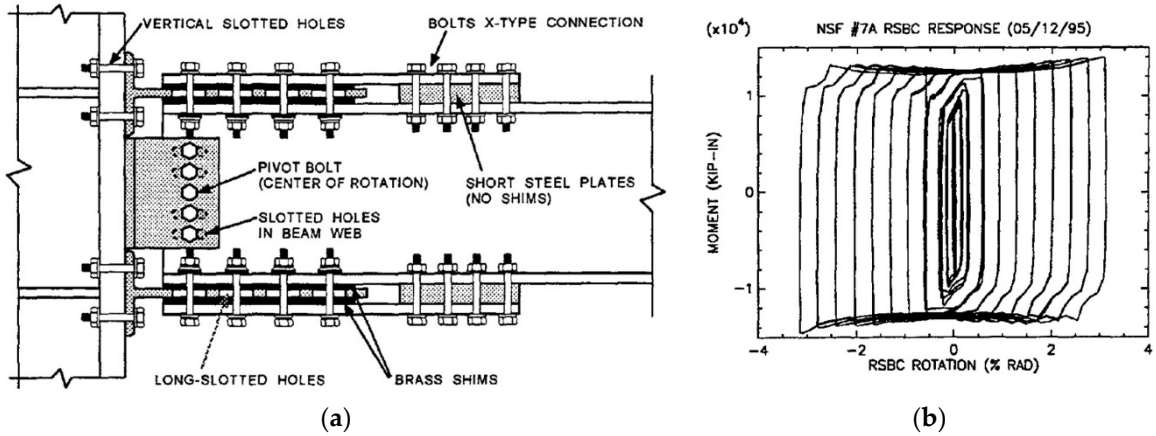

(**a**) (**b**)

Figure 1. (a) Symmetric connections with two or more friction shims per side: Rotational Slotted Bolted Connection (RSBC) (b) RSBC experimental moment-rotation curve (taken from [37]).

3. Sliding Hinge Joint with Asymmetric Friction Connection

Among the most recent connections developed at the University of Auckland and University of Canterbury plays an important role the connection that belongs to the first group, which is named Sliding Hinge Joint with Asymmetric Friction Connection (SHJAFC) shown in Figure 2 [38–40].

The solution solves two main drawbacks affecting the RSBC, namely the center of rotation constituted by a pivot bolt, to which particular attention has to be paid during structural design to avoid any damage to the bolt itself and to the plates connected by it, and the gap opening between top flange of beam and column flange, which could potentially lead to damage of the slab. In this solution, the beam is connected to the column by means of two horizontal steel plates, which are welded to the column flange next to the beam. The connection between these steel plates and the beam is made with bolts, where the upper ones realize a standard bolted friction connection, while the lower ones are inserted through slotted holes to allow the rotation of the beam. Between the bottom beam flange and the lower plate is inserted a friction shim, which provides adequate dissipative capacity to the connection.

A cap plate is bolted to the bottom side of the lower plate, inserting between the latter ones another friction shim. A vertical plate is welded to the column flange and bolted to the beam web by means of two horizontal rows of bolts. The top one is a standard bolted connection, while the bottom one is characterized by horizontal slotted holes to allow the rotation of the beam. Moreover, with the aim of increasing the dissipative capacity of the connection, a cap plate is bolted to the outer side of the web plate. Between the cap plate and web plate, and between the web plate and the beam web two friction shims are inserted.

The connection starts to rotate when the friction forces provided by the shims inserted between bottom beam flange and bottom plate, beam web and web plate, are achieved. Increasing the rotation of the system, the total friction force doubles when the friction shims inserted between the bottom and web plates and the cap plates begin to slide (Figure 3).

 doi:10.20944/preprints202312.1958.v1

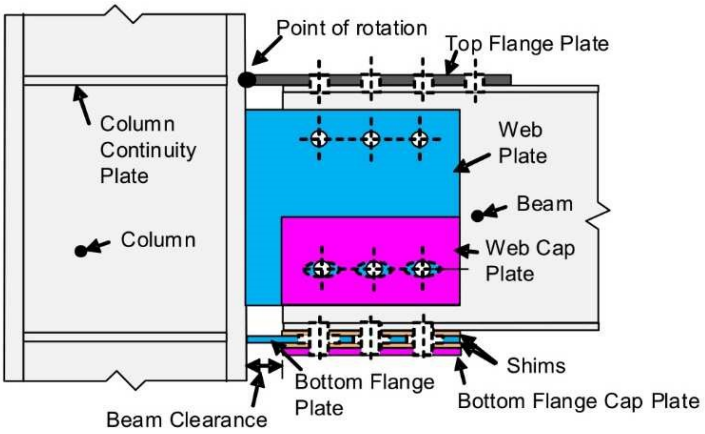

Figure 2. Asymmetric connections with one or more friction shims: Sliding Hinge Joint (SHJ) (taken from [39].

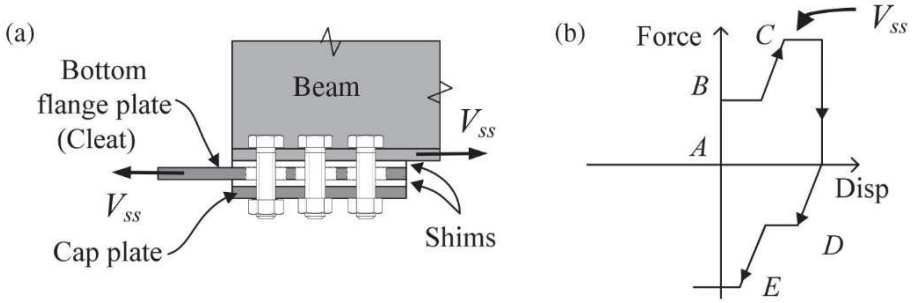

Figure 3. (a) Asymmetric Friction Connection (AFC) (b) its moment-rotation curve (taken from [39]).

During the design step of the SHJAFC, special attention must be paid to the Serviceability Limit State and to the wind loads. As a matter of fact, due to the above-mentioned moment-rotation behavior, the connection could start to rotate when subjected to loads different from those caused by the design earthquake. Furthermore, the asymmetric arrangement of the friction device leads to bolts contemporarily subjected to moment, shear and axial load, which, in early versions of this connection, caused plastic deformations of bolts shanks. This phenomenon decreased clamping force leading to hysteretic cycles characterized by a progressive reduction of the sliding force. To solve this issue, bolts have to be kept within the elastic range and coupled with disc springs able to absorb the elongation undergone by bolts shanks [41].

When SHJAFC is endowed with friction pads having a hardness much higher than that of constructional steel, it provides wide and stable hysteretic cycles, with a slight progressive increase of sliding force (Figure 4). This phenomenon is due to the formation of asperities on the surfaces in contact.

From the pioneering configurations developed at the end of the last century, during the last decade the Sliding Hinge Joint SHJ has been further developed in order to be self-centering [42,43]. This behavior is obtained by adding at the bottom beam flange a stack of preloaded ring springs inserted in a box-shaped case. A bar is inserted through the ring springs and is bolted to the column flange. The system is designed to deform the ring springs in compression only for both hogging and sagging moment (Figure 5).

Experimental tests carried out on different combinations of moment strength provided by the AFC and the stack of disc springs pointed out that the more is the percentage of moment strength provided by the AFC on the whole moment strength of the connection the less is the self-centering capacity of the connection itself.

For instance, in Figure 6 is shown the moment rotation curve of a self-centering SHJAFC characterized by a percentage of moment capacity provided by preloaded ring springs P_{RS} of 52.4%. It can be seen that, despite P_{RS} being more than half of the whole moment capacity of the connection, significant residual drift was still obtained. Therefore, P_{RS} should be increased by using a more

 doi:10.20944/preprints202312.1958.v1

performing and thus more expensive self-centering system. In addition, the connection behaved according to design requirements for rotation up to 25 mrad.

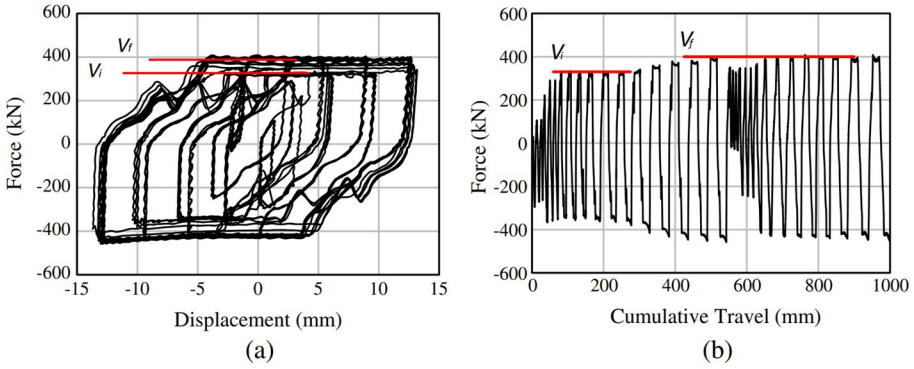

Figure 4. (a) Asymmetric Friction Connection force-displacement curve (b) and force-cumulative travel (b) (taken from [39]).

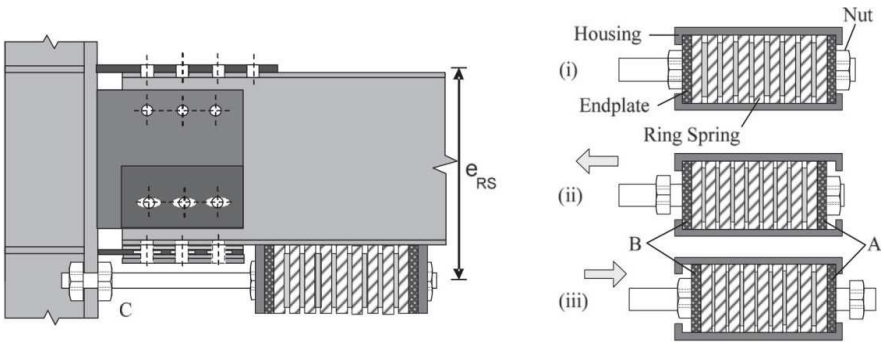

Figure 5. Self-centering Sliding Hinge Joint (SCSHJ) (taken from [43]).

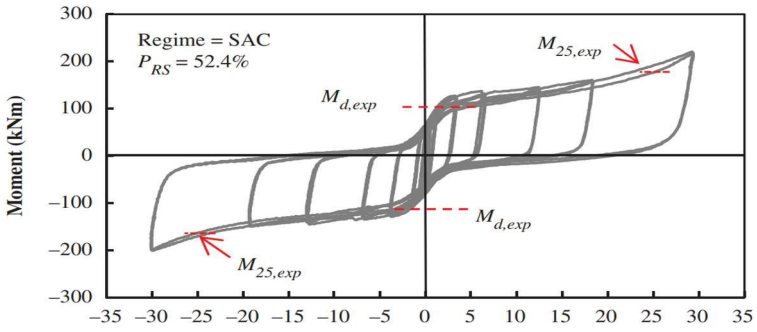

Figure 6. SCSHJ experimental moment-rotational curve (taken from [43]).

Above this value, the vertical component of the displacement due to the rotation was no longer negligible and the moment strength increased rapidly. This is due to the fact that the connection was not designed to accommodate large displacement in the vertical direction, thus some damage could have been experienced by the connection. Moreover, in the case of seismic events leading to rotation well above 25 mrad, the increment in the moment strength of the connection could have led to the formation of plastic hinge at the beam end or, worse, to damaging the column. For this reason, a real application of this connection should select an appropriate overstrength factor to design the members surrounding the connection to prevent any damage.

 doi:10.20944/preprints202312.1958.v1

4. Dissipative Double Split Tee Connection

A solution belonging to the second group has been developed at the University of Salerno, Italy, and it is named Dissipative Double Split Tee Connection (DDSTC) [44]. The connection is made with two T stubs, bolted to the beam flanges, on which slotted holes are realized to allow the sliding of the bolts (Figure 7). Between the T stub and beam flange is inserted a friction shim, which provides energy dissipation capacity. The connection is designed in order to allow the vertical component of the displacement due to the rotation by means of the deflection of T stubs. The latter ones are supposed to undergo plastic deformations at the base section and then to be replaced after the seismic event. This configuration does not have a defined center of rotation, leading to potential significant damage to the slab.

Experimental tests have shown remarkable performance characterized by an adequate dissipative capacity and a slight hardening behavior due to bending moment acting on T stubs flanges, as already seen in the RSBC (Figure 8). The solution simplifies the configuration of the RSBC by removing cap plates and pivot bolt.

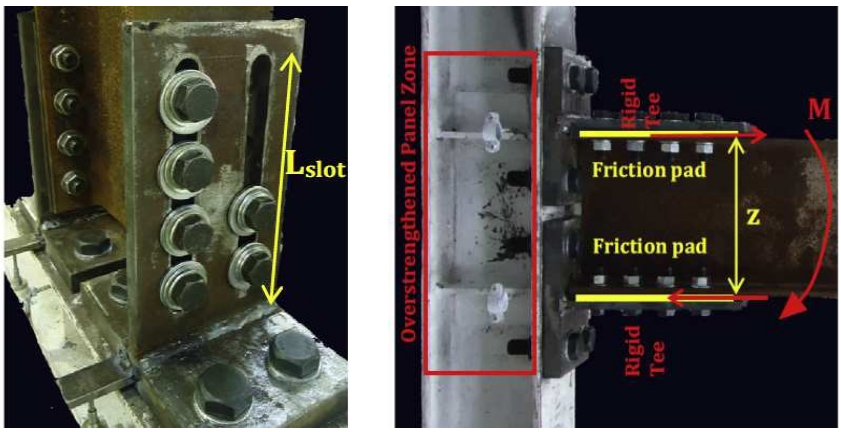

Figure 7. Asymmetric connections with one friction shim per side: Dissipative Double Split Tee Connection (DDSTC) (a) Bottom View (b) Side View (taken from [44]).

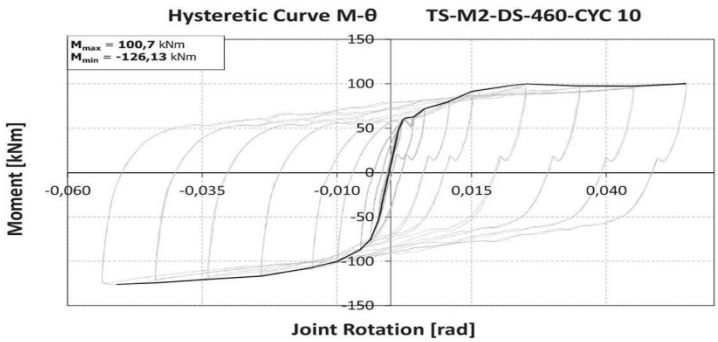

Figure 8. DDSTC experimental moment-rotation curve (taken from [44]).

The reduction of number of surfaces on which friction forces are generated, which would lead to a lower moment capacity of the connection, is compensated by using friction shims having higher friction coefficient. However, by doing so the friction connections become asymmetric and the bolts are subjected to combined axial force-shear force-bending moment that, as discussed in the SHJAFC, might lead to plastic deformations of bolts shanks, potentially causing decreasing clamping forces and poor cyclic performance of the connection.

[45] did an experimental campaign on asymmetric beam to column joint and derived an analytical model based on the component method [46]. The main aim of this research was to predict

 doi:10.20944/preprints202312.1958.v1

the cyclic behavior of partial-strength beam-to-column joints which helps the designers to correctly analyze the non-linear response of connections in seismic time-history analyses, and to precisely predict the degradation of the slip properties of friction joints.

The tested beam-to-column joint is like a conventional double split tee connection. However, some modifications are done. In double traditional double split tee connections, the bottom T stub is used to connect the lower flange to the column face; but here replaced with a friction device having possibility of two different geometrical configurations as shown in Figure 9.

In the configuration 1 (Figure 9a) the symmetrical friction dampers are parallel to the beam flange. Here, the device consists of friction pads, 10.9 high strength preloaded bolts, a couple of L stubs, and a slotted stainless-steel haunch which permits the sliding of the device. The L stubs connect the assembly to the column flange, helps the transfer of bolt forces and clamp the friction shims and the haunch together.

In the second configuration 2 (Figure 9b), there is a relative movement of L stubs and rib plates in friction shims which produce the sliding, so all of these elements are with slotted holes.

The friction device consists of stainless-steel plate (lower part of the haunch in configuration 1 and rib plate in configuration 2). One of the interesting things is that the damper performs same in both cases but relative decrease or increase of the bolt preloading forces can occur for configuration 1 due to the flexibility of the L stubs and rigid beam rotation, and vice versa for configuration 2 as the variation of bolt forces doesn't exist because it does not depend on the L stubs deformation.

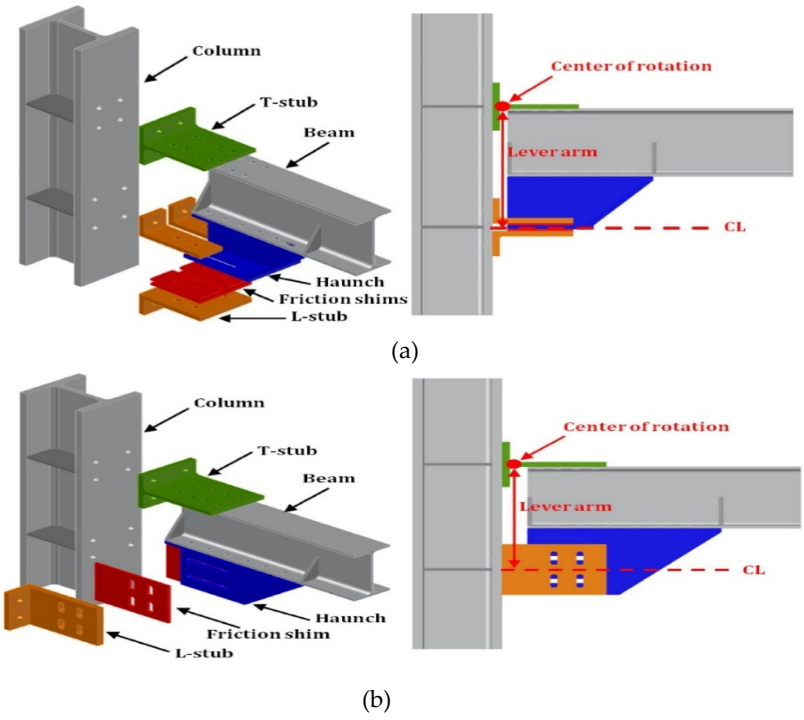

Figure 9. (a) Damper plane parallel to beam flange (configuration 1) (b) Damper plane parallel to beam web (configuration 2) (taken from [45])

The experimental analysis confirmed that the response of configuration (1) joint was asymmetric, and it causes the fluctuations of the bolt preloading forces. The reason is due to the different deformability of the L stubs in tension/compression and due to the uneven distribution of pressures in the friction interface because of the due to the compatibility between the bending of L stub and joint rotation in configuration (1).

Results also show that in configuration (2), the friction joints are less prone to variation of bolt forces variations which shows less asymmetric response as compared to configuration (1).

When the specimen is of cruciform the asymmetry disappears at the same time because at the same nodal point, one of the connections is under sagging bending moment while other is in hogging.

 doi:10.20944/preprints202312.1958.v1

So, it can be analyzed that locally the behavior of friction joints is of some asymmetry while overall the MRF response will always be symmetrical for any direction of the seismic force because of the same number of connections in hogging and sagging bending.

5. Removable Friction Dampers for Low-Damage Connections

The same Authors, in collaboration with the University of Naples "Federico II", Italy, propose two other solutions, one with the dissipative friction sliding plates in horizontal direction, the other one with friction sliding plates oriented in vertical direction, belonging to the third group [47,48]. These solutions aim at solving three main flaws of the previous solution, i.e., the lack of a center of rotation, the asymmetric configuration of the friction connections, and the relatively small moment capacity, which is due to a combination of small internal lever arm of the connection and small number of friction surfaces for each side (i.e., equal to 1).

Both of these solutions exploit an additional steel element which is bolted to the bottom beam flange with the aim of increasing the internal lever arm of the connection and, thus, reducing the forces acting on the panel zone. This additional steel element is an I-shaped profile in case of horizontal dissipative device, while is T-shaped in case of vertical one.

Another advantage provided by the additional steel element is that it allows to double the surfaces on which friction forces are generated, considerably improving the performance of the connections. The upper part of the beam is connected to the column flange by means of a T stub which is bolted to both the column and the beam. In both the solutions, the center of rotation is expected to form at the base section of the upper T stub. The solution with the horizontal dissipative device is constituted by three steel angles which are bolted to the I-shaped profile, using one friction pad for each steel angle (Figure 10).

Figure 10. Symmetric connections with additional steel element(s) and two or more friction shims arranged horizontally (taken from [47]).

On the other hand, the solution with the vertical dissipative device employs two steel angles, requiring the realization of two groups of slotted holes, one vertically oriented on the steel angles, and the other one horizontally oriented on the T-shaped profile (Figure 11). By doing so, bolts are able to move in any direction. By contrast, in the solution with horizontal dissipative device, the displacement component in vertical direction is absorbed by the deformation of the lower steel angles. Differently from the horizontal system, in which low damage of the lower steel angles is admitted, the vertical one prevents any damage of the friction connection. However, bolts belonging to the friction device experience plastic deformations due to the contact between horizontal slotted holes of the T-shaped profile and bolts shanks. In fact, these bolts have to be dragged up and down by the T-shaped profile, along the vertical direction, in order to allow the rotation of the connection.

 doi:10.20944/preprints202312.1958.v1

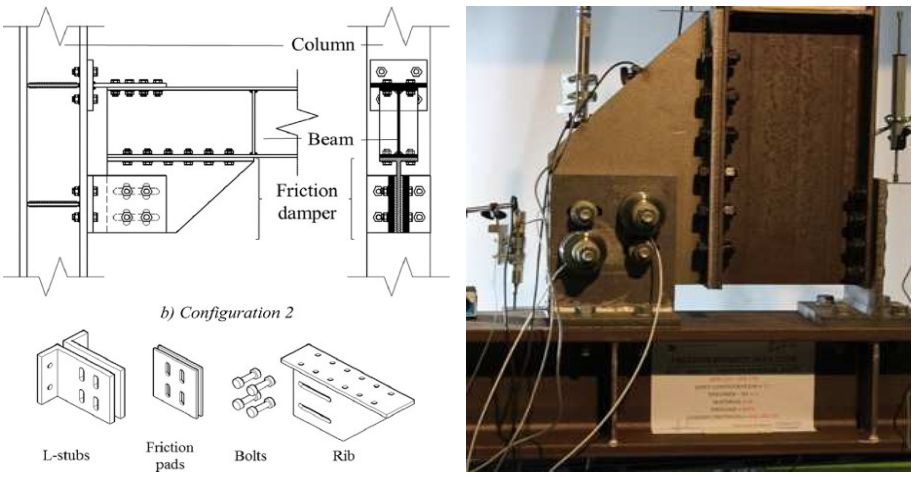

Figure 11. Symmetric connections with additional steel element(s) and two or more friction shims arranged vertically (taken from [48]).

With regard to the mechanical behavior, the horizontal system shows an increment of the moment capacity, in both directions, due to the progressive plasticization of the lower steel angles (Figure 12a). As for the vertical system, the contact between bolts shanks and horizontal slotted holes causes an increment of the moment capacity which depends on the amount of bolts shanks dragged by the T-shaped profile. For this reason, the backbone curve of the moment rotation behavior showed a sawtooth-like shape (Figure 12b).

Moment capacity increment due to these phenomena has to be properly taken into account when designing the members connected to the friction connection with the aim of avoiding damage formation.

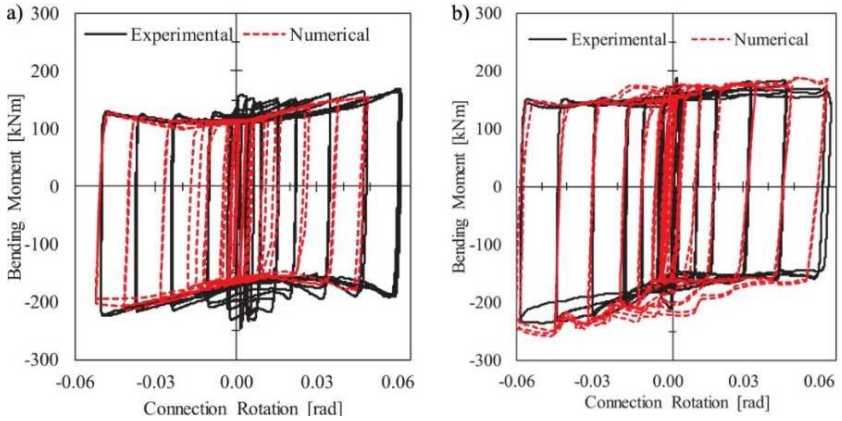

Figure 12. (a) Moment-rotation behavior of the horizontal system (b) the vertical system (taken from [48]).

Therefore, it is worth outlining the design procedure of the above connection.

The force F_d for which the connection starts to slide can be calculated as follows:

$$F_d = M_d / z \quad (1)$$

in which M_d is the design bending moment and z is the lever arm, being the distance between the center of rotation and the axis of sliding. According to [46], the sliding force F_d can be obtained as:

$$F_d = (K_s n_b n_s \mu / \gamma_{M3}) * F_{pc} \quad (2)$$

where, K_s = coefficient that depends on the shape of the slotted hole, n_b = the number of bolts, n_s = the number of surfaces in contact, μ = the friction coefficient, γ_{M3} = safety factor, F_{pc} = preloading force of each bolt. The F_{pc} can be assessed as follows:

 doi:10.20944/preprints202312.1958.v1

$$F_{pc} = 0.7\ ts\ f_{ub}\ A_{res} \quad (3)$$

where, f_{ub} = ultimate strength of steel, A_{res} = resisting area of bolt, while t_s = a parameter ranging between 0.3 and 0.6, introduced to keep bolt within the elastic range and, thus, limit preload losses due to creep phenomena [49,50].

[51] did a parametric study by using the finite element simulation and modelling of a steel beam to column joint. To this aim a set of five friction dampers based on the steel profiles used in Eurocode-compliant multi-storey moment resisting frames have been used shown in (Figure 13). Experimental tests were performed in the previous study [48] and the FEM models were calibrated against those tested before.

The aim of this research was to extend the findings of experimental results, investigating the behavior of different damping connections. The surface interaction of plate to plate and bolt to plate were modelled using the tangential and normal behavior. For the normal, "Hard Contact" is taken while for tangential is modelled different for friction pads to steel and steel to steel interfaces.

For friction dampers the dynamic friction coefficient is taken as 0.59 [52] and for steel-to-steel surface taken as 0.3. Pre-tensioning of bolts were done in order to applied bolt preload according to the recommendation of EN1993 1–8 [46]. The column was allowed to deform along its own axis by pinning it at the bottom end and by all flexural rotations as well as the vertical displacements at the upper end. The beam tip was simply pinned while it was restrained lateral-torsional buckling in accordance with [46]. Both cyclic and monotonic displacement histories were applied at the beam tip according to the [53].

The following results can be derived by the simulations.

- The rotational capacity and ductility of the friction connection is dependent on some of the factors like the lever arm of joint, the length of the slotted holes in the rib and the gap between the beam's tip and column flange, which refrains the contact between the connected members under hogging flexure, while permits the plastic hinge formation at the base of the T stub web

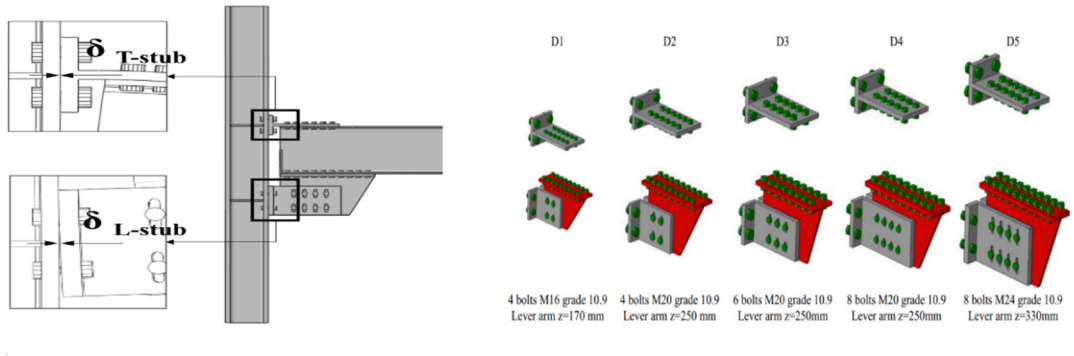

(**a**) (**b**)

Figure 13. (a) L stub configuration (b) Five symmetric friction dampers with their configuration (taken from [51]).

- It was found that the effectiveness of friction joints isn't dependent on the size of connected members because the hysteretic and monotonic response of all joints was almost the same
- The friction dampers and connections give the rotation capacity of about 0.07 rad, which fulfills the minimum rotation capacity criteria given [54,55] for dissipative joints
- The flexural response of the joints having the proposed dampers is not symmetric, and for the chord rotation of 0.04 rad the hogging resistance is about 25% greater than the sagging one. It is mainly due to the higher deformability of the L stubs under sagging moment which causes the higher loss of bolt preload as compared to the loss when the L stubs are in compression.

 doi:10.20944/preprints202312.1958.v1

In order to find the seismic response of Low damage/FREEDAM joints [31] tested a large scale two-storey building mock-up having two equal frames equipped with low-damage FREEDAM joints having friction dampers as shown in Figure 14.

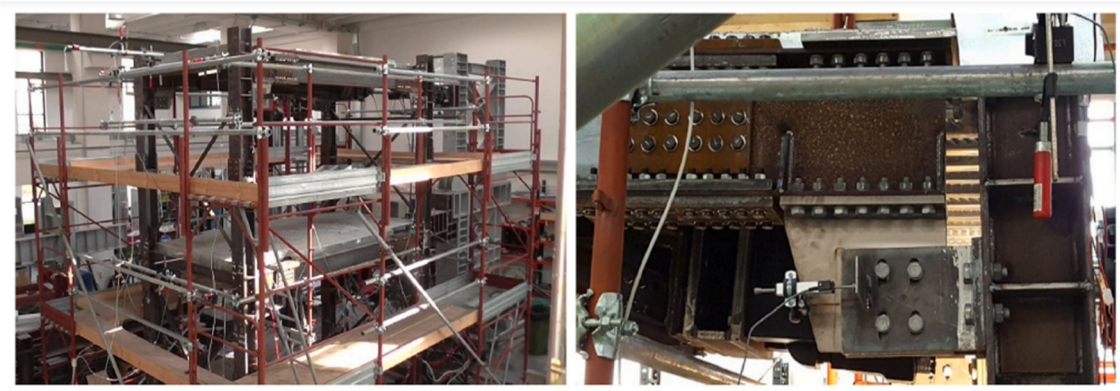

(**a**) (**b**)

Figure 14. (a) Tested moment resisting frame equipped with FREEDAM joint (b) Configuration of tested FREEDAM joint (taken from [31]

To simulate the seismic event effects, a sequence of five accelerograms has been applied by pseudo dynamic testing. The geometrical details of tested FREEDAM joint are shown in Figure 15.

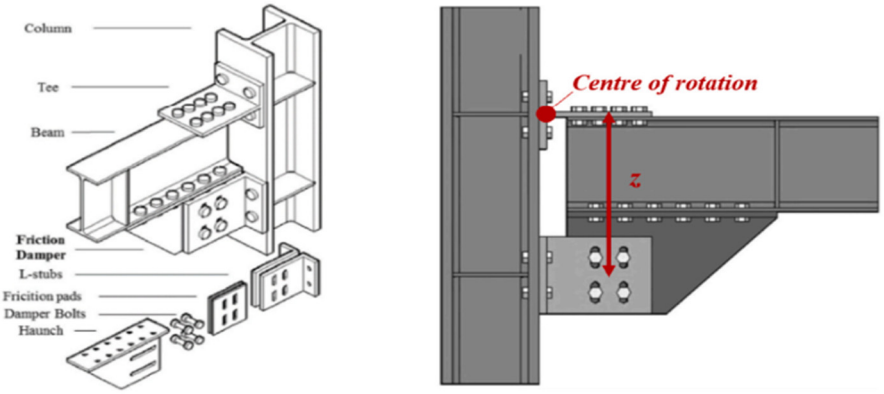

Figure 15. Geometrical configuration and details of low damage design (FREEDAM) joint (taken from [31]).

The experimental results confirmed that low yielding friction joints provide enough energy dissipation and rotation supply without any damage. These experimental results have been verified by a numerical method.

It was also found that the connection didn't suffer any damage but there was a minor yielding which is same as of the results previously tested by [56] on beam-to-column joints sub-assemblages. Friction pads at the end of tests need to be repaired because of the friction and energy dissipation. There was a little degradation of connection's flexural resistance during the experimental campaign which proves that friction pads can resist the seismic event, but anyway minor repair may still be needed.

The friction-based beam to column connection proposed in [34,57,58] it is the only one in the literature designed for the connection of RC columns cast in situ connected with HSTCBs. The need to design such a device was highlighted by experimental tests conducted on traditional connections between RC columns and HSTCB, which highlighted the loss of stiffness caused by cracking of the

 doi:10.20944/preprints202312.1958.v1

joint panel in connections with beams characterized by a high percentage of longitudinal reinforcement [59].

The device was designed to connect an HSCTB having dimensions of = 300 x 250 mm^{2,} longitudinal rebars of 4ϕ24 (top) + 2ϕ24 (bottom), taking advantage of the steel plate on the bottom side of the beam that act as a mold in the casting phase, and as reinforcing element at the Serviceability Limit States (SLS) and Ultimate Limit States (ULS). The transverse reinforcement of beam was ϕ8/6 cm. A relevant issue in the design of the devices was the shear strength that have to be provided to the beam, that was calculated as 350 kN using the analytical model of [60], which develops that proposed in [61].

The device specimen is represented in Figure 16b; the T stub is made of HEB300 profile, and the connection between T stub and HSTCB was made with eight M20 bolts class 10.9 while between the column and T stub is made of four M24 bolts class 10.9. The steel angles were coated with thermal sprayed aluminum and used as friction pads, as shown in Figure 16c. Thermal sprayed aluminum was chosen as friction material based on its best performance as tested by [35]. The connection between the thermal sprayed aluminum steel angles and vertical central plate was made by five M20 bolts class 10.9 and the thermal sprayed aluminum steel angles were connected with column with four M24 bolts class 10.9. An axial load of 500 kN was applied on the column to simulate the effect of dead load.

Displacement controlled tests were carried out by applying on the HSTCB at a distance from the center of rotation of l = 1.31 m. The displacement history was considered as suggested by ACI 374.2R-13 (2013) [62]. Two cycles of five amplitudes of maximum displacement of ± 2 mm, ± 5 mm, ± 10 mm, ± 20 mm and ± 40 mm were applied.

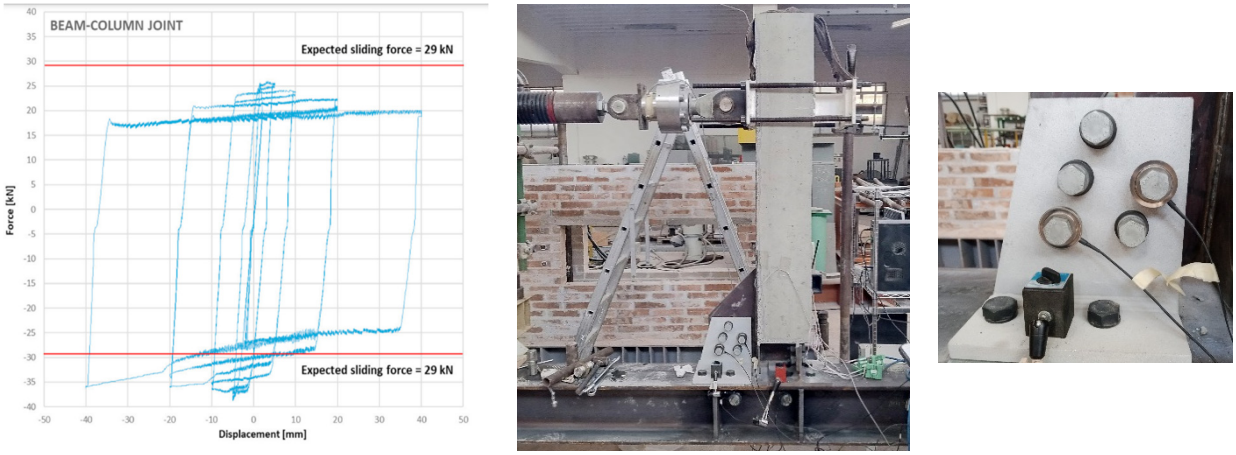

(**a**) (**b**) (**c**)

Figure 16. (a) Force Displacement curve of HSTCB and column with friction dissipative device (taken from [35]) (b) Specimen endowed with friction device (c) Friction device.

Several tests were performed, with joint strength equal to 0.35, 0.5, 1, 1.5 of the ultimate bending strength of the HSTCBs, equal to 105 kN-m. In Figure 16a the result of the test with the lower strength, namely 36.75 kN-m is reported, where a torque was applied on the bolts to achieve a preload of 17 kN, and expected sliding force, equal to F_{sl} = 29kN. The results showed that beam-column connection provides stable and wide hysteresis loops without any damage or cracking. There were different values of the sliding force in the case of sagging moment and hogging moment due to change of lever arm. It was also found that the sliding force reduce during the test because of the wearing of surface and loss of preload force due to stick and slip phenomenon.

 doi:10.20944/preprints202312.1958.v1

6. Self-Centering Friction Connection for PC MRFs

As underlined in the introduction, in order to obtain devices that guarantee full functionality of the structure after the earthquake, a significant characteristic of the device is the recentering capacity. In the literature various devices are designed according to the methods that characterize the re-centering behavior of the device proposed in [63–65]. The device shown in Figure 17, was developed for Precast Concrete (PC) structures, and belongs to the fourth group.

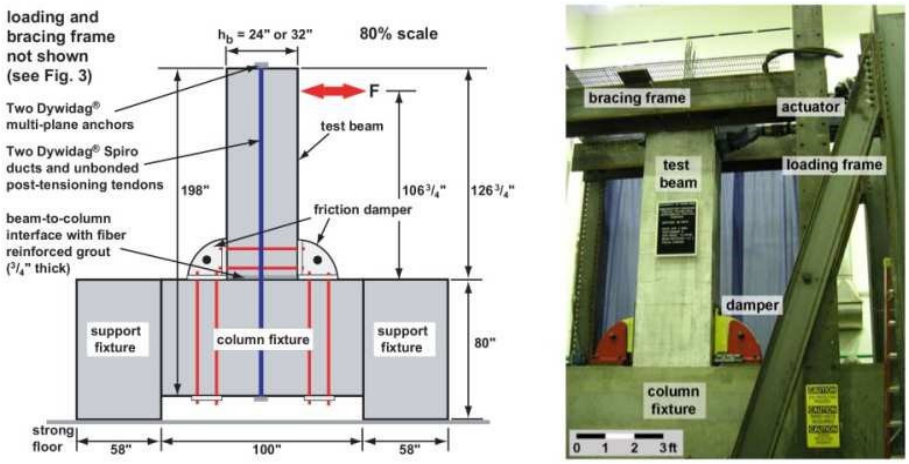

Figure 17. Symmetric connections with two or more friction shims per side for PC structures (taken from [63]).

The connection between column and beam is made using only two bolts, both inserted through curved slotted holes. Each dissipative device is constituted by four friction shims (Figure 18).

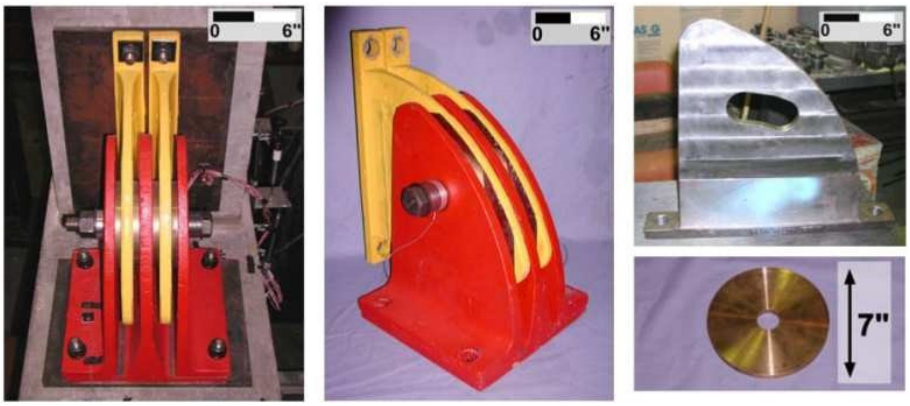

Figure 18. Friction device layout (taken from [63]).

Beam and column are connected with one or more unbounded post-tensioned tendons, which are positioned at the mid height of the beam cross-section, providing self-centering behavior to the connection. In Figure 19 are represented the theoretical moment-rotation curve of the self-centering connection, as well as the contribution provided by friction devices and post-tensioned tendons. The latter is characterized by a bilinear- elastic behavior, in which moment value M_{bp} is tuned by means of preload force acting on the tendons, while second branch stiffness is ruled by axial stiffness of tendons. It should be noted that the theoretical contribution given by post-tensioned tendons does not dissipate energy, these behaving elastically.

Yet, this is not fully confirmed by experimental tests, as can be seen in Figure 20, in which are reported two moment-rotation curves of a subassembly endowed with post-tensioned tendons and including or not friction dampers. In both cases, the more was the rotation achieved by the

 doi:10.20944/preprints202312.1958.v1

connection, the less was the moment value for which the gap at beam-column interface opens (i.e., without dampers equals to M_{bp}, Figure 20a; with dampers equals to M_{bd}, Figure 20b.

This phenomenon was due to concrete cracking and crushing at interface between beam and column, being the latter ones in contact. As a matter of fact, this contact is required to transfer the shear force between beam and column, otherwise, in the presence of friction connections, these would withstand this force and their functioning would be hampered.

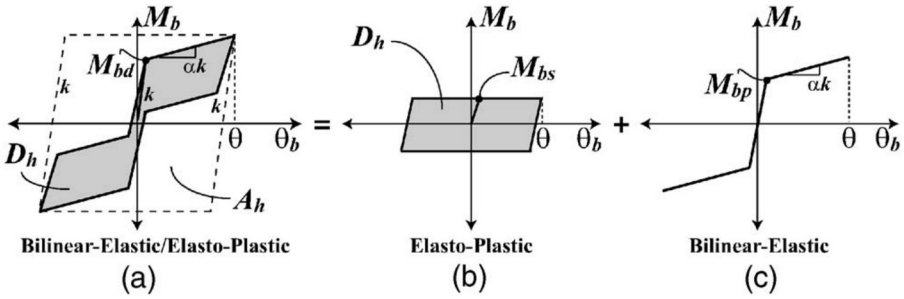

Figure 19. Theoretical moment-rotation curves of: (a) self-centering friction connection (b) friction dampers only (c) post-tensioned tendons only (c) (taken from [64]).

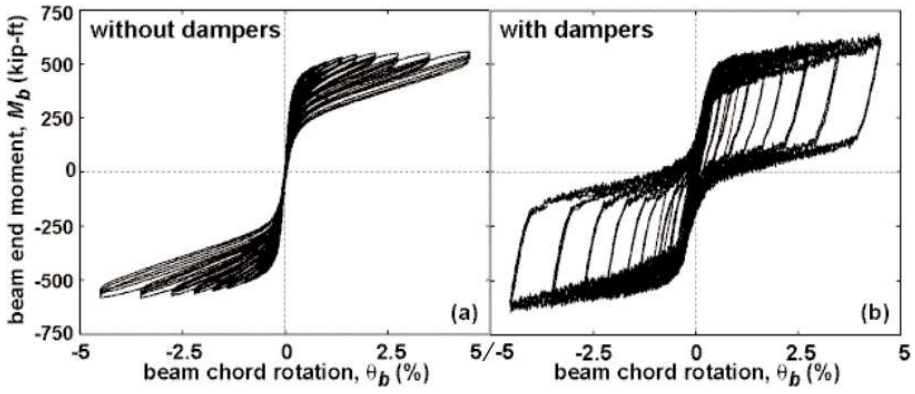

Figure 20. Experimental moment-rotation curve of the beam-column joint endowed with (a) post-tensioned tendon only (b) and coupled with friction dampers (taken from [63]).

Moreover, progressive damage of concrete leads also to hysteretic cycles with small amplitude in the case of subassembly without dampers. On a final note, the results provided by post-tensioned tendons are promising in terms of dissipative and self-centering capacities. However, it has to be stressed that this structural typology requires to tension the tendons in the construction site once the PC members are placed, limiting its use to relevant constructions only.

7. Common Issues Affecting Friction Connections

To obtain an optimal behavior for friction devices with low slipping strength, it is very important to have stable friction coefficient (CoF) between the friction dampers interfaces, and a precise control over the value and the variation of bolt preload. Thus, all the above-mentioned structural solutions are highly influenced by two issues:

- characteristics of friction shim
- values and control of bolt preload.

As for the first one, since the research of [15] where simple bolted steel plate is adopted, or [16] where the behavior of asbestos brake lining pads was investigated, over the last four decades many research groups have focused their attention on the research of materials whose characteristics are optimal for this type of use. Recently, in [66], the behavior of six distinct couplings of materials were analyzed, namely steel–steel, brass–steel, sprayed aluminum–steel and three interfaces implementing

 doi:10.20944/preprints202312.1958.v1

distinct friction rubber-based materials. In Figure 21, a typical experimental test for the assessment of the friction properties of materials is illustrated. The specimen is constituted by two steel plates, one with normal clearance hole and the other one with slotted holes, connected by means of a double cover butt joint. Between the two steel plates and the cover plates are inserted two friction shims. The test is carried out by imposing to one of the two steel plates a displacement history.

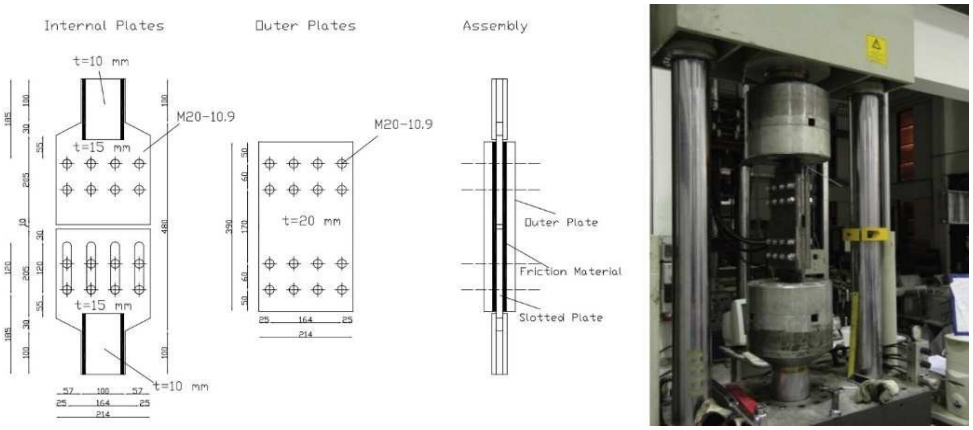

Figure 21. Typical experimental test for the assessment of the friction properties of materials (taken from [66]).

For instance, in Figure 22, the force displacement curve of a specimen employing non-superficially treated steel as friction shims is reported.

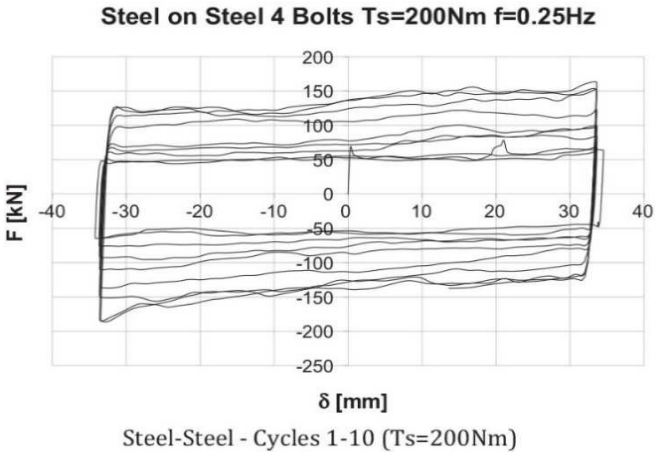

Figure 22. Force-displacement curve of a specimen employing non-superficially-treated steel as friction shims (taken from [66]).

It can be noticed that, by increasing the number of cycles, the required force to activate the slippage of the slotted steel plate increased considerably, tripling the initial value during the last cycles. This phenomenon was due to the increasing roughness of the surfaces in contact, which led to a higher friction coefficient. On the other hand, when superficially treated steel is used as friction shims, the test outcomes can be the opposite, i.e., flattening of the superficial asperities which leads to a lower friction coefficient and, consequently, to a decreasing resistance of the friction connection. It is clear that these phenomena may hamper the cyclic behavior of dissipative friction connections.

For this reason, the optimal friction material has to provide a high friction coefficient in order to maximize the connection performance, and whose value remains stable during the cycles. Moreover, materials which might show relaxing phenomena (e.g., polymeric) should be avoided. Lastly, material durability must be taken into account, because the environmental conditions in which the connection is used could change the material properties during its life cycle.

 doi:10.20944/preprints202312.1958.v1

Regarding the second issue, i.e., bolt preload, this is influenced by the procedure used to apply the preload and short- and long-term loss of preload. As a matter of fact, by using the common procedures to apply the preload (e.g., torque method) it is impractical to apply exactly the required preload. In Figure 23, the effective preload applied to a group of 15 bolts M20 class 10.9 is shown. The applied preload is measured by using a donut cell load between the bolt head and the steel plate through which the bolt is inserted. As can be seen, the variation is remarkable, having preloads at fractiles 95% and 5% equal to 212 kN and 182 kN, respectively. Therefore, such a variation of bolt preload affects the cyclic behavior of friction connections. Other than the above-mentioned uncertainties, many studies have investigated the short and long-term loss of bolt preload, which are mainly due to creep phenomena and flattening of asperities of the surfaces in contact. With the purpose of minimizing these issues, as already mentioned before, several authors e.g., [49,50] suggest limiting the bolt preload between 30% and 60% of the maximum value calculated by means of [46].

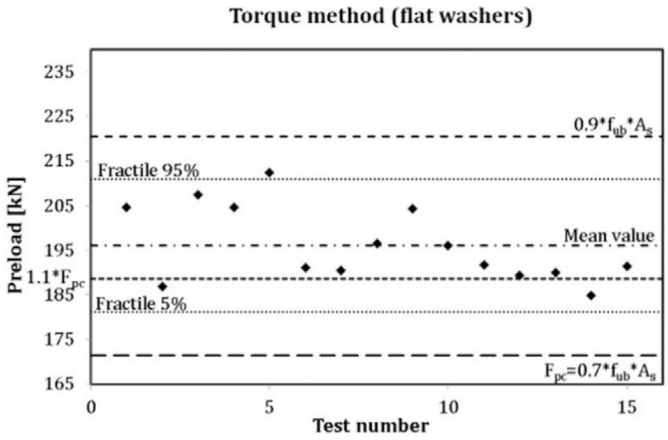

Figure 23. Effective preload applied to a group of 15 bolts M20 class 10.9 (taken from [50]).

In order to achieve stable friction coefficient (CoF) between the friction dampers interfaces, and a precise control over the value and the variation of bolt preload [67] worked on innovative friction materials having stable hysteretic response along with higher, less varied friction coefficient and predictable/stable slip resistance. The internal surface of the device was realized from stainless steel AISI 304 (chosen for its corrosion resistance) having a superficial hardness of roughly 130 HV, while a coupled material that exhibits a higher superficial hardness was chosen. To analyze the variation of friction coefficient of the tested materials, the experimental layout is taken as same as mirrored in [50]. To this aim, the uniaxial device shown in Figure 24 has been tested. Specifically, it was connected to the testing machine via a slotted plate made of AISI 304 stainless steel and a steel plate. Pre-stressed external steel plates and friction pads were bolted to these plates using assemblies composed of M20 class 10.9 High strength bolts and washers. Friction value, along with its degradation over time was determined. The bolt preload values were calibrated at 60% of the proof preloading load. The load protocol was taken as according to EN15129 [68], and the specimens underwent testing involving a cyclic loading process conducted in three stages, progressively increasing to 25%, 50%, and 100% of the device's maximum design displacement.

 doi:10.20944/preprints202312.1958.v1

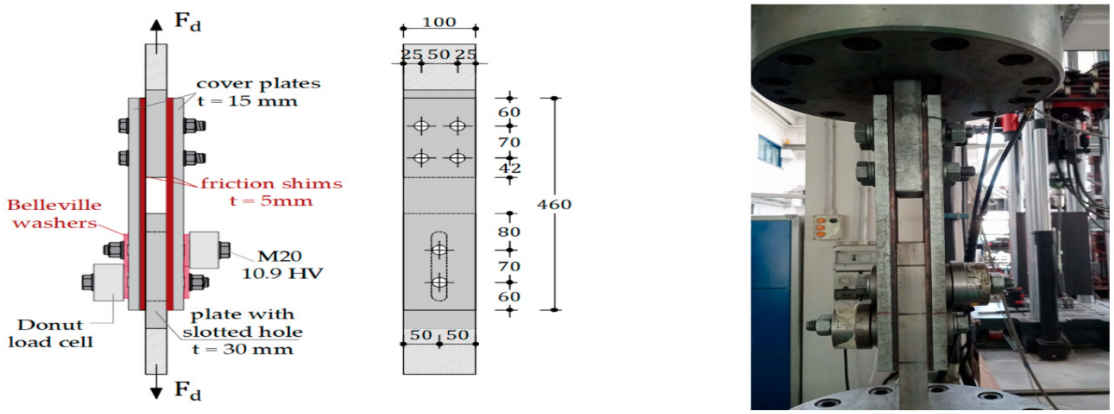

(**a**) (**b**)

Figure 24. (a) Geometrical details of uniaxial friction device (b) Tested Specimen (taken from [67]).

Initial tests indicate that, regardless of the surface treatment technique used for the friction surfaces, there is no considerable increase in the performance of the friction devices. On the contrary, when assessing an unproven device, hysteric behavior is considerably more stable, showing a resistance degradation of less than 15%. This enhancement is due to a combination of a friction coefficient with a nearly constant value throughout the entire test, due to a more cohesive interface between the two friction faces during earlier testing, and minimal preload losses in the bolts. This conclusion is verified by an analysis of hysteretic behavior by various test configurations, including the analysis of degradation of actual and effective friction coefficients. As a matter of fact, for an unsuitable choice of the material coupled at the friction damper interface, at the end of the test a value that has tripled compared to the value recorded at the beginning of the test was exhibited.

[35] did an experimental study and FEM analysis on uniaxial dissipative devices with different types of friction materials i.e., steel, brass and thermal sprayed aluminum. The main aim of the research was to analyze the dissipative capacity, to check the variation of friction coefficient, and to find the effect of disc springs and bolt preload variation. The tested specimen was configured similar to that proposed by [66] as shown in Figure 25. It is composed of upper and bottom two central steel plates of S355 profile having thickness of 15mm, one plate is with standard clearance holes and other is with slotted holes. Two friction pads are sandwiched on both sides of plates with cover plates. Six M12 class 10.9 bolts are used on the fixed side and four preloaded bolts are on the other sliding side. The design of this uniaxial device was done according to [69]. The device was tested under cyclic displacements of 7.5mm, 15mm and 30mm. 40% of code consistent bolt preload (24kN) was applied on each bolt.

The experiment results revealed that the thermal sprayed aluminum has a constant friction coefficient after some starting number of cycles. The coefficient remains between 0.57 to 0.6 and less bolt preload variation occurs because of the presence of disc springs. While, when brass was used as a friction material large fluctuations of bolt preload and friction coefficient were observed. The results proved that thermal sprayed aluminum friction pads provide higher energy dissipation and stable results as compared to brass. FEM analysis has been done to verify the effectiveness of uniaxial dissipative device and ability of disc springs. The results also confirmed the effectiveness of uniaxial devices in terms of energy dissipation and proved that the disc springs are necessary in order to refrain the variation of bolt preload and maintenance of contact pressure.

 doi:10.20944/preprints202312.1958.v1

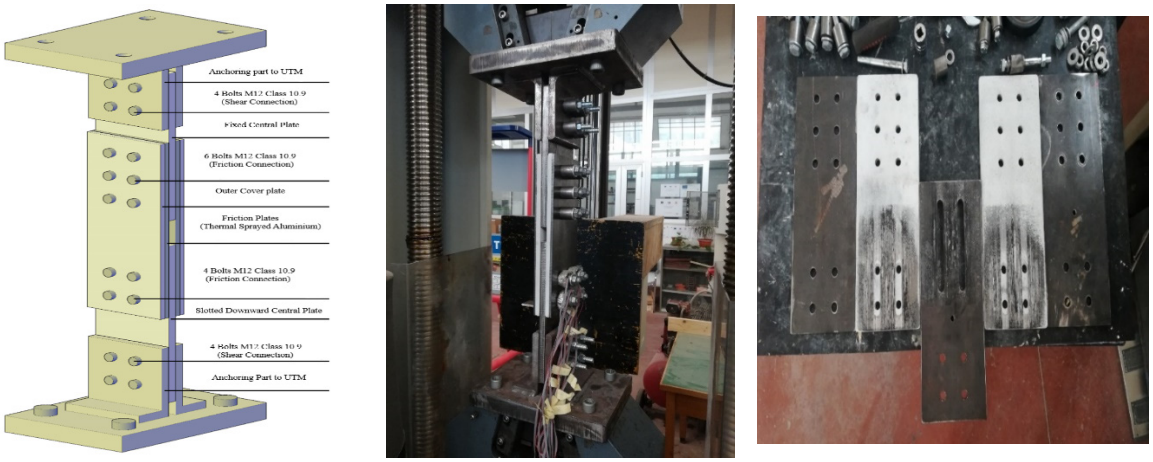

(**a**) (**b**) (**c**)

Figure 25. (a) Geometrical details of uniaxial friction device (b) Tested Specimen (c) Thermal sprayed aluminum and cover plates after test (taken from [35]).

8. Conclusions

On the basis of the analysis of the solutions found in the literature, the following considerations are drawn, which can be used to define the solutions for the beam-to-column connections, that are the aims of the present research.

- symmetric dissipative system ensures a stable response in terms of bending moment capacity, at the same time reducing the stresses experienced by the bolts
- steel angles connected to the vertical dissipative device remain within the elastic range, simplifying the constructional system with respect to the horizontal dissipative device
- T stubs and/or L stubs of horizontal dissipative device(s) provide a bending moment contribution during sliding phase
- the vertical dissipative device, as arranged by [47], exhibits an undesired contribution as well, provided by the bolts of friction device that have to be dragged up and down during the sliding phase
- the dissipative device used only at the lower part of the beam does not interfere with the other layers at the upper part of the beam, reducing or avoiding the damaging of the slab
- the kinematic behavior of the beam-to-column connection is predictable only if it is known as prior to the position of the center of rotation
- separating the beam end section and the column face prevents that damage that can occur at this interface.

Among the several solutions presented in this section, those developed by [47,48], might be seemed as the most balanced ones, being characterized by wide and stable hysteresis loops, bolts subjected to symmetric forces, ease of realization, and cost-effectiveness. SHJ is an unquestionably excellent solution for beam-to-column connection, and the AFC compactness does not introduce any obstacle to architectural layout design. However, doubling of the sliding force during the functioning of the connection raises some concerns during the design procedure. In addition, the asymmetric configuration of the friction device calls for paying particular attention to the design of bolts. In fact, these are subjected to combined axial force, shear force and bending moment, and bolts shanks are particularly prone to plastic deformations. However, the latter should be avoided since they could reduce clamping force of bolts and thus, deteriorate the cyclic performance of the connection.

Regarding the self-centering version of the SHJAFC, it seems to provide effective performance which is linked to a significative increment of cost of the whole connection. Despite of their promising results, the use of friction connections coupled with unbounded post-tensioned tendons in PC

structures requires specific procedures during construction process, which could significantly rise construction costs and make competitive using other structural typologies of recentering system.

Regarding the tribological properties of the materials at the interface of the sliding surfaces, researchers have demonstrated that steel on steel interface showed a high friction coefficient, but a quite variable behavior, with an initial hardening phase, followed by a rapid decay of the friction coefficient. Steel on brass interface shown a stable behavior but characterized by low friction coefficient. Steel on thermal sprayed aluminum is characterized by high value of the friction coefficient, and a stable behavior if the surface is initially treated to reduce the irregular asperity due to manual spraying process, minimizing the variability of the friction coefficient with respect to the applied pressure.

Regarding the application and the control of bolt preload, research has shown that this is influenced by the procedure used to apply the preload, short and long-term loss of preload. By using the common procedures to apply the preload (e.g., torque method) it is impractical to apply exactly the required preload. In order to ensure minimum dispersion of the applied compressive load, it is recommended to strictly define the torque application procedure, the type of bolts used, and the materials at the interface of the sliding surfaces and at the bolt, washer, plate interface, the type of disc spring used, and perform experimental tests for the statistical characterization of the applied preload.

However, bolt preload is also affected by short and long term loss mainly due to creep phenomenon and flattening of asperities of the surfaces in contact, that are almost unpredictable also, but they can be efficiently limited both by the use of disc spring, and limiting the bolt preload between 30% and 60% of the maximum value calculated by means of EN 1993:1-8.

Author Contributions: Conceptualization, bibliographic researches, methodology, writing—original draft preparation, and review and editing, were performed by all authors with the same contribution; funding acquisition, Piero Colajanni. All authors have read and agreed to the published version of the manuscript.

Funding: The studies presented here were carried out as part of the activities envisaged by the RETURN Extended Partnership and received funding from the European Union Next-Generation EU (National Recovery and Resilience Plan – NRRP, Mission 4, Component 2, Investment 1.3 – D.D. 1243 2/8/2022, PE0000005).

Institutional Review Board Statement: Not applicable

Informed Consent Statement: Not applicable

Data Availability Statement: The data presented in this study are available on request from the corresponding author

Conflicts of Interest: The authors declare no conflict of interest.

References

1. Housner, George W. "Limit design of structures to resist earthquakes." In *Proc. World Conference of Earthquake Engineering, 1956. 6*. 1956.
2. Kelly, J.M. Aseismic Base Isolation: Review and Bibliography. *Soil Dynamics and Earthquake Engineering* **1986**, *5*, 202–216, doi:10.1016/0267-7261(86)90006-0.
3. Cacciola, P.; Tombari, A. Vibrating Barrier: A Novel Device for the Passive Control of Structures under Ground Motion. *Proc. R. Soc. A.* **2015**, *471*, 20150075, doi:10.1098/rspa.2015.0075.
4. Colajanni, P.; Papia, M. Hysteretic Behavior Characterization of Friction-Damped Braced Frames. *J. Struct. Eng.* **1997**, *123*, 1020–1028, doi:10.1061/(ASCE)0733-9445(1997)123:8(1020).
5. Akiyama, H. *Earthquake-Resistant Limit-State Design for Buildings*; University of Tokyo press, 1985; ISBN 4-13-068111-7.
6. Skinner, R.I.; Kelly, J.M.; Heine, A.J. Hysteretic Dampers for Earthquake-resistant Structures. *Earthq Engng Struct Dyn* **1974**, *3*, 287–296, doi:10.1002/eqe.4290030307.
7. Cao, X.-Y.; Shen, D.; Feng, D.-C.; Wang, C.-L.; Qu, Z.; Wu, G. Seismic Retrofitting of Existing Frame Buildings through Externally Attached Sub-Structures: State of the Art Review and Future Perspectives. *Journal of Building Engineering* **2022**, *57*, 104904, doi:10.1016/j.jobe.2022.104904.

8. Benfratello, S.; Cucchiara, C.; Palizzolo, L.; Tabbuso, P. Fixed Strength and Stiffness Hinges for Steel Frames. In Proceedings of the AIMETA 2017-Proceedings of the 23rd Conference of the Italian Association of Theoretical and Applied Mechanics; Centro Servizi d'Ateneo Srl, 2017; Vol. 1, pp. 1287–1296.
9. Benfratello, S.; Caddemi, S.; Palizzolo, L.; Pantò, B.; Rapicavoli, D.; Vazzano, S. Targeted Steel Frames by Means of Innovative Moment Resisting Connections. *Journal of Constructional Steel Research* **2021**, *183*, 106695, doi:10.1016/j.jcsr.2021.106695.
10. Benfratello, S.; Palizzolo, L.; Vazzano, S. A New Design Problem in the Formulation of a Special Moment Resisting Connection Device for Preventing Local Buckling. *Applied Sciences* **2021**, *12*, 202, doi:10.3390/app12010202.
11. Jaisee, S.; Yue, F.; Chen, L.; Yin, W.; Gong, H.; Wang, C. Shaking Table Investigations on the Seismic Performance of a Steel Frame with Optimized Passive Energy Dissipation Devices. *IOP Conf. Ser.: Earth Environ. Sci.* **2019**, *330*, 022081, doi:10.1088/1755-1315/330/2/022081.
12. Jaisee, S.; Yue, F.; Ooi, Y.H. A State-of-the-Art Review on Passive Friction Dampers and Their Applications. *Engineering Structures* **2021**, *235*, 112022, doi:10.1016/j.engstruct.2021.112022.
13. Janke, L.; Czaderski, C.; Motavalli, M.; Ruth, J. Applications of Shape Memory Alloys in Civil Engineering Structures—Overview, Limits and New Ideas. *Materials and structures* **2005**, *38*, 578–592.
14. Higazey, M.M.; Alshannag, M.J.; Alqarni, A.S. Numerical Investigation on the Performance of Exterior Beam–Column Joints Reinforced with Shape Memory Alloys. *Buildings* **2023**, *13*, 1801, doi:10.3390/buildings13071801.
15. Pall, A.S.; Marsh, C.; Fazio, P. Friction Joints for Seismic Control of Large Panel Structures. *pcij* **1980**, *25*, 38–61, doi:10.15554/pcij.11011980.38.61.
16. Pall, A.S.; Marsh, C. Response of Friction Damped Braced Frames. *J. Struct. Div.* **1982**, *108*, 1313–1323, doi:10.1061/JSDEAG.0005968.
17. Pasquin, C.; Leboeuf, N.; Pall, R.T.; Pall, A. Friction Dampers for Seismic Rehabilitation of Eaton's Building, Montreal. In Proceedings of the 13th world conference on earthquake engineering; 2004; pp. 1–2.
18. Chen, W.-F.; Lui, E.M. *Handbook of Structural Engineering*; CRC press, 2005; ISBN 1-4200-3993-8.
19. Roh, J.-E.; Hur, M.-W.; Choi, H.-H.; Lee, S.-H. Development of a Multiaction Hybrid Damper for Passive Energy Dissipation. *Shock and Vibration* **2018**, *2018*, 1–16, doi:10.1155/2018/5630746.
20. Soong, T.T.; Dargush, G.F. *Passive Energy Dissipation Systems in Structural Engineering*; J. Wiley & sons: Chichester New York Weinheim, 1997; ISBN 978-0-471-96821-4.
21. Symans, M.D.; Charney, F.A.; Whittaker, A.S.; Constantinou, M.C.; Kircher, C.A.; Johnson, M.W.; McNamara, R.J. Energy Dissipation Systems for Seismic Applications: Current Practice and Recent Developments. *J. Struct. Eng.* **2008**, *134*, 3–21, doi:10.1061/(ASCE)0733-9445(2008)134:1(3).
22. Perkowski, W. DRY FRICTION DAMPER FOR SUPERCRITICAL DRIVE SHAFT. *Journal of KONES. Powertrain and Transport* **2016**, *23*, 389–396, doi:10.5604/12314005.1217255.
23. Pesaresi, L.; Stender, M.; Ruffini, V.; Schwingshackl, C.W. DIC Measurement of the Kinematics of a Friction Damper for Turbine Applications. In *Dynamics of Coupled Structures, Volume 4*; Allen, M.S., Mayes, R.L., Rixen, D.J., Eds.; Conference Proceedings of the Society for Experimental Mechanics Series; Springer International Publishing: Cham, 2017; pp. 93–101 ISBN 978-3-319-54929-3.
24. Csaba, G. Modelling of a Microslip Friction Damper Subjected to Translation and Rotation. In Proceedings of the Volume 4: Manufacturing Materials and Metallurgy; Ceramics; Structures and Dynamics; Controls, Diagnostics and Instrumentation; Education; IGTI Scholar Award; General; American Society of Mechanical Engineers: Indianapolis, Indiana, USA, June 7 1999; p. V004T03A012.
25. Sanati, M.; Khadem, S.E.; Mirzabagheri, S.; Sanati, H.; Khosravieh, M.Y. Performance Evaluation of a Novel Rotational Damper for Structural Reinforcement Steel Frames Subjected to Lateral Excitations. *Earthq. Eng. Eng. Vib.* **2014**, *13*, 75–84, doi:10.1007/s11803-014-0213-5.
26. Lee, C.-H.; Kim, J.; Kim, D.-H.; Ryu, J.; Ju, Y.K. Numerical and Experimental Analysis of Combined Behavior of Shear-Type Friction Damper and Non-Uniform Strip Damper for Multi-Level Seismic Protection. *Engineering Structures* **2016**, *114*, 75–92, doi:10.1016/j.engstruct.2016.02.007.
27. Kim, J.; Shin, H. Seismic Loss Assessment of a Structure Retrofitted with Slit-Friction Hybrid Dampers. *Engineering Structures* **2017**, *130*, 336–350, doi:10.1016/j.engstruct.2016.10.052.
28. Titirla, M.D.; Papadopoulos, P.K.; Doudoumis, I.N.; Katakalos, K.V. Cyclic Response of an Antisesmic Steel Device for Building–an Experimental and Numerical Study. In Proceedings of the 16TH World Conference on Earthquake Engineering; 2017; pp. 9–13.

29. Titirla, M.D.; Papadopoulos, P.K.; Doudoumis, I.N. Finite Element Modelling of an Innovative Passive Energy Dissipation Device for Seismic Hazard Mitigation. *Engineering Structures* **2018**, *168*, 218–228, doi:10.1016/j.engstruct.2018.04.081.
30. Bagheri, S.; Barghian, M.; Saieri, F.; Farzinfar, A. U-Shaped Metallic-Yielding Damper in Building Structures: Seismic Behavior and Comparison with a Friction Damper. *Structures* **2015**, *3*, 163–171, doi:10.1016/j.istruc.2015.04.003.
31. Di Benedetto, S.; Francavilla, A.B.; Latour, M.; Piluso, V.; Rizzano, G. Experimental Response of a Large-Scale Two-Storey Steel Building Equipped with Low-Yielding Friction Joints. *Soil Dynamics and Earthquake Engineering* **2022**, *152*, 107022, doi:10.1016/j.soildyn.2021.107022.
32. Hashemi, A.; Zarnani, P.; Masoudnia, R.; Quenneville, P. Seismic Resistant Rocking Coupled Walls with Innovative Resilient Slip Friction (RSF) Joints. *Journal of Constructional Steel Research* **2017**, *129*, 215–226, doi:10.1016/j.jcsr.2016.11.016.
33. Belleri, A.; Marini, A.; Riva, P.; Nascimbene, R. Dissipating and Re-Centering Devices for Portal-Frame Precast Structures. *Engineering Structures* **2017**, *150*, 736–745, doi:10.1016/j.engstruct.2017.07.072.
34. Pagnotta, S.; Monaco, A.; Colajanni, P.; La Mendola, L. Experimental Characterization of Friction Properties of Materials for Innovative Beam-to-Column Dissipative Connection for Low-Damage RC Structures. *Procedia Structural Integrity* **2023**, *44*, 1909–1916, doi:10.1016/j.prostr.2023.01.244.
35. Pagnotta, S.; Ahmed, M.; Colajanni, P. EXPERIMENTAL AND FINITE ELEMENT ANALYSIS OF THE CYCLIC BEHAVIOR OF LINEAR DISSIPATIVE DEVICES.; Athens, Greece, 2023; pp. 3077–3090.
36. Grigorian, C.E. *Energy Dissipation with Slotted Bolted Connections*; University of California, Berkeley, 1994; ISBN 9798208467978.
37. Yang, T.-S. Experimental and Analytical Studies of Steel Connections and Energy Dissipators; University of California, Berkeley, 1995; ISBN 9798209343059.
38. Chanchi Golondrino, J.C.; MacRae, G.A.; Chase, J.G.; Rodgers, G.W.; Clifton, G.C. Asymmetric Friction Connection (AFC) Design for Seismic Energy Dissipation. *Journal of Constructional Steel Research* **2019**, *157*, 70–81, doi:10.1016/j.jcsr.2019.02.027.
39. Khoo, H.; Clifton, C.; MacRae, G.; Zhou, H.; Ramhormozian, S. Proposed Design Models for the Asymmetric Friction Connection. *Earthq Engng Struct Dyn* **2015**, *44*, 1309–1324, doi:10.1002/eqe.2520.
40. Ramhormozian, S.; Clifton, G.C.; MacRae, G.A.; Khoo, H.H. The Sliding Hinge Joint: Final Steps towards an Optimum Low Damage Seismic-Resistant Steel System. *KEM* **2018**, *763*, 751–760, doi:10.4028/www.scientific.net/KEM.763.751.
41. Ramhormozian, S.; Clifton, G.C.; MacRae, G.A.; Davet, G.P. Stiffness-Based Approach for Belleville Springs Use in Friction Sliding Structural Connections. *Journal of Constructional Steel Research* **2017**, *138*, 340–356, doi:10.1016/j.jcsr.2017.07.009.
42. Khoo, H.-H.; Clifton, C.; Butterworth, J.; MacRae, G.; Gledhill, S.; Sidwell, G. Development of the Self-Centering Sliding Hinge Joint with Friction Ring Springs. *Journal of Constructional Steel Research* **2012**, *78*, 201–211, doi:10.1016/j.jcsr.2012.07.006.
43. Khoo, H.-H.; Clifton, C.; Butterworth, J.; MacRae, G. Experimental Study of Full-Scale Self-Centering Sliding Hinge Joint Connections with Friction Ring Springs. *Journal of Earthquake Engineering* **2013**, *17*, 972–997, doi:10.1080/13632469.2013.787378.
44. Latour, M.; Piluso, V.; Rizzano, G. Free from Damage Beam-to-Column Joints: Testing and Design of DST Connections with Friction Pads. *Engineering Structures* **2015**, *85*, 219–233, doi:10.1016/j.engstruct.2014.12.019
45. Latour, M.; Santos, A.F.; Santiago, A.; Ferrante Cavallaro, G.; Piluso, V. Component Modelling of Low-Damage Beam-to-Column Joints Equipped with Friction Dampers. *Structures* **2022**, *46*, 1561–1580, doi:10.1016/j.istruc.2022.10.095.
46. CEN, E. 1-8. Eurocode 3: Design of Steel Structures: Part 1.8: Design of Joints, 2005. *European Committee for Standardization: Bruxelas* **1993**.
47. Latour, M.; Piluso, V.; Rizzano, G. Experimental Analysis of Beam-to-Column Joints Equipped with Sprayed Aluminum Friction Dampers. *Journal of Constructional Steel Research* **2018**, *146*, 33–48, doi:10.1016/j.jcsr.2018.03.014.
48. Latour, M.; D'Aniello, M.; Zimbru, M.; Rizzano, G.; Piluso, V.; Landolfo, R. Removable Friction Dampers for Low-Damage Steel Beam-to-Column Joints. *Soil Dynamics and Earthquake Engineering* **2018**, *115*, 66–81, doi:10.1016/j.soildyn.2018.08.002.

49. Ferrante Cavallaro, G.; Francavilla, A.; Latour, M.; Piluso, V.; Rizzano, G. Experimental Behavior of Innovative Thermal Spray Coating Materials for FREEDAM Joints. *Composites Part B: Engineering* **2017**, *115*, 289–299, doi:10.1016/j.compositesb.2016.09.075.
50. Ferrante Cavallaro, G.; Latour, M.; Francavilla, A.B.; Piluso, V.; Rizzano, G. Standardised Friction Damper Bolt Assemblies Time-Related Relaxation and Installed Tension Variability. *Journal of Constructional Steel Research* **2018**, *141*, 145–155, doi:10.1016/j.jcsr.2017.10.029.
51. Tartaglia, R.; D'Aniello, M.; Campiche, A.; Latour, M. Symmetric Friction Dampers in Beam-to-Column Joints for Low-Damage Steel MRFs. *Journal of Constructional Steel Research* **2021**, *184*, 106791, doi:10.1016/j.jcsr.2021.106791.
52. Zimbru, M.; D'Aniello, M.; Martino, A.D.; Latour, M.; Rizzano, G.; Piluso, V. Investigation on Friction Features of Dissipative Lap Shear Connections by Means of Experimental and Numerical Tests. *TOBCTJ* **2018**, *12*, 154–169, doi:10.2174/1874836801812010154.
53. ANSI/AISC 341-16 Seismic Provisions for Structural Steel Buildings. *Seismic Provisions for Structural Steel Buildings* **2016**, 60601.
54. EN, C. 1 (2004) Eurocode 8: Design of Structures for Earthquake Resistance—Part 1: General Rules, Seismic Actions and Rules for Buildings. *European Committee for Standardization (CEN), Brussels* **1998**.
55. CEN EN 1998–1, Design of Structures for Earthquake Resistance - Part 1: General Rules, Seismic Actions and Rules for Buildings, 2005.
56. Francavilla, A.B.; Latour, M.; Piluso, V.; Rizzano, G. Design Criteria for Beam-to-Column Connections Equipped with Friction Devices. *Journal of Constructional Steel Research* **2020**, *172*, 106240, doi:10.1016/j.jcsr.2020.106240.
57. Colajanni, P.; Pagnotta, S. Friction-Based Beam-to-Column Connection for Low-Damage RC Frames with Hybrid Trussed Beams. *Steel and Composite Structures* **2022**, *45*, 231–248, doi:10.12989/SCS.2022.45.2.231.
58. Colajanni, P.; La Mendola, L.; Monaco, A.; Pagnotta, S. Low-Damage Friction Connections in Hybrid Joints of Frames of Reiforced-Concrete Buildings. *Applied Sciences* **2023**, *13*, 7876, doi:10.3390/app13137876.
59. Colajanni, P.; La Mendola, L.; Monaco, A.; Spinella, N. Cyclic Behavior of Composite Truss Beam-to-RC Column Joints in MRFS. *KEM* **2016**, *711*, 681–689, doi:10.4028/www.scientific.net/KEM.711.681.
60. Colajanni, P.; Pagnotta, S.; Recupero, A.; Spinella, N. Shear Resistance Analytical Evaluation for RC Beams with Transverse Reinforcement with Two Different Inclinations. *Mater Struct* **2020**, *53*, 18, doi:10.1617/s11527-020-1452-8.
61. Colajanni, P.; Recupero, A.; Spinella, N. Shear Strength Degradation Due to Flexural Ductility Demand in Circular RC Columns. *Bull Earthquake Eng* **2015**, *13*, 1795–1807, doi:10.1007/s10518-014-9691-0.
62. American Concrete Institute Committee 374. *ACI374.2R-13: Guide for Testing Reinforced Concrete Structural Elements under Slowly Applied Simulated Seismic Loads*; ACI: Farmington Hills, MI, USA, 2013.1.
63. Morgen, B.G.; Kurama, Y.C. A Friction Damper for Post-Tensioned Precast Concrete Moment Frames. *pcij* **2004**, *49*, 112–133, doi:10.15554/pcij.07012004.112.133.
64. Morgen, B.G.; Kurama, Y.C. Seismic Design of Friction-Damped Precast Concrete Frame Structures. *J. Struct. Eng.* **2007**, *133*, 1501–1511, doi:10.1061/(ASCE)0733-9445(2007)133:11(1501).
65. Morgen, B.G.; Kurama, Y.C. Seismic Response Evaluation of Posttensioned Precast Concrete Frames with Friction Dampers. *J. Struct. Eng.* **2008**, *134*, 132–145, doi:10.1061/(ASCE)0733-9445(2008)134:1(132).
66. Latour, M.; Piluso, V.; Rizzano, G. Experimental Analysis on Friction Materials for Supplemental Damping Devices. *Construction and Building Materials* **2014**, *65*, 159–176, doi:10.1016/j.conbuildmat.2014.04.092.
67. Francavilla, A.B.; Latour, M.; Rizzano, G. Prototype Test of Resilient Friction Materials for Seismic Dampers. *Materials* **2023**, *16*, 7336, doi:10.3390/ma16237336.
68. *CEN* 15129; Anti-Seismic Devices. European Committee for Standardization: Brussels, Belgium, 2009.
69. En, B. 1-1, Eurocode 3: Design of Steel Structures: Part 1-1: General Rules and Rules for Buildings. *European Committee for Standardization* **2005**.